High-Performance Vitrimer Entailing Renewable Plasticizer Engineered for Processability and Reactivity toward Composite Applications

Lorenz, Niklas; Dyer, William E.; Kumru, Baris

Important note
To cite this publication, please use the final published version (if applicable).
Please check the document version above.

Article

High-Performance Vitrimer Entailing Renewable Plasticizer Engineered for Processability and Reactivity toward Composite Applications

Niklas Lorenz,* William E. Dyer, and Baris Kumru

Cite This: *ACS Appl. Polym. Mater.* 2025, 7, 1934−1946

Read Online

ACCESS | Metrics & More | Article Recommendations | SI Supporting Information

ABSTRACT: The present article introduces a high-performance epoxy vitrimer to target structural composite applications. By utilizing a reactive diluent derived from biobased feedstock, the maximum glass transition is tailored to maintain a sufficient temperature window for reprocessing, avoiding the degradation of permanent bonds. Different fractions of permanent cross-links are imbued into the network structure, and the hybrid network is elucidated by creep and stress relaxation. The creep behavior at service temperatures below 150 °C remains unaffected, while slower bond exchange dynamics and higher extrapolated topology freezing temperatures T_v are reported for an increasing number of permanent cross-links. Comprehensive studies of physicochemical, thermo-rheological, and curing reactions are carried out and summarized in a conversion-temperature phase diagram first reported for a vitrimer. The vitrimers show great malleability, even with permanent cross-link fractions above the theoretical limit for a percolated network formation, and we demonstrate recycling by comminuting and subsequent reconsolidation. These findings provide valuable guidance for enhancing material and process development of high-performance vitrimer resins and lay the groundwork for advancing composites built on vitrimer matrix systems.

KEYWORDS: *vitrimer, disulfide, epoxy, hybrid networks, liquid composite molding, characterization*
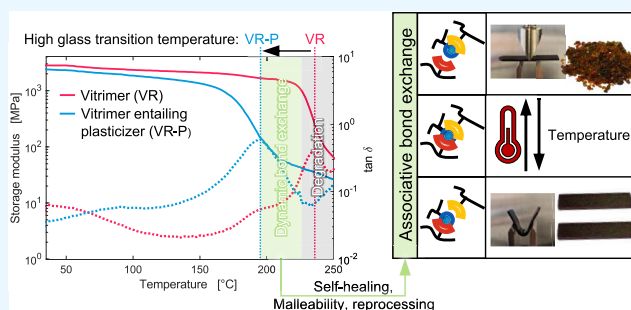
1. INTRODUCTION

Epoxy resins are vital thermosetting polymers that are widely utilized across numerous industries and everyday applications. Their remarkable characteristics, including superior dimensional and thermal stability, high mechanical strength, resistance to creep, excellent electrical insulation, and strong chemical resistance, make them indispensable in various sectors such as automotive, aerospace, and electronic devices.[1] At the same time, due to their three-dimensional cross-linked nature, epoxy resins cannot be recycled, reformed, or dissolved once cured,[2] rendering them less eco-friendly than thermoplastics and resulting in substantial end-of-life (landfill) waste. The primary disposal methods for thermoset resins and composites, such as pyrolysis and landfilling, pose significant environmental and economic challenges.[3]

The integration of covalent adaptive networks (CANs) into epoxy systems has introduced a novel class of polymers by enhancing thermoset properties with exceptional features like recyclability, malleability, and self-healing characteristics— previously associated only with thermoplastics.[4] This novel class, known as vitrimers, offers an alternative to conventional epoxy resins, providing the potential for sustainable use through comprehensive recycling strategies and extended service life via self-healing capabilities.[1,5] Indeed, vitrimers

show promise for replacing traditional thermosetting materials in various industries, paving the way for more sustainable material production. However, research on vitrimers for specific applications is still in its early stages.[4,6]

Besides introduction of dynamic cross-links, renewable feedstock-based materials are gaining interest to attain sustainability aims, e.g., by closed-loop recyclability.[7] Reactive diluents obtained from a renewable feedstock can show promising results by replacing the petrochemicals, thus supporting sustainability by low volatility and nontoxicity.[8] Further, the essential characteristic (imparting lower viscosity to resin) can be beneficial to overcome the higher viscosity of disulfide-based vitrimer resin formulations as observed in refs 5,9,10. In particular, the combination of dynamic bonding and renewable feedstock-based materials seems a convincing approach to overcome the plastic pollution problems of
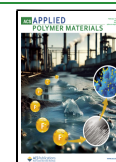
conventional synthetic thermoset and thermoplastic polymer materials.

However, it is not easily feasible to directly replace a resin system with a more sustainable alternative. Especially, in the aerospace industry, epoxy resins are difficult to replace due to their good thermal and mechanical properties. Besides that, the certification process for novel aerospace materials tends to be very time- and cost-intensive.[6] For a variety of aerospace applications, high glass transition temperatures ($T_g \geq 180$ °C) represent a pivotal requirement to consider. It is common practice to establish the material operational limit by reducing the T_g by a prescribed value, typically 28 °C (50 °F), below the measured glass transition temperature.[11] It seems challenging to fulfill these requirements with vitrimers, as the majority focusing on epoxy resins with exchangeable disulfide cross-links report maximum T_g in the range of 131−163 °C.[12−14] Only a few studies have reported that the requirement of a high T_g demanded for aerospace applications can be met[15,16] reporting a maximum T_g of 233 °C.[9] However, some of the beneficial properties of the vitrimers are sacrificed: No reconsolidation of the comminuted material can be present in ref 9 as the processing region overlaps with the degradation of the disulfide bonds. A small reduction in T_g was observed in ref 16 during comminuting and reconsolidation which the authors attributed to possible breakage of the nonreversible bonds due to comminuting process and high-temperature reprocessing. In ref 15, the authors bypass this drawback by inserting a dynamic transesterification reaction facilitating the hydrolysis of ester bonds in the network, enabling degradation in pure water at 200 °C. Still, the properties resulting from the bond exchange dynamics, such as malleability and healing properties, were not studied in detail. Thus, for disulfide-based vitrimer systems, there seems to be a threshold of T_g (assuming significant dynamic bond exchange can only occur at $T > T_g$) above which the benefit of dynamic bond exchange is affected by thermal degradation which is already observed at temperatures above 200 °C although it depends heavily on the period of exposure.[17,18]

Besides that, dimensional stability is one of the most important properties of solid materials for long-term operation, but few materials are perfect in this respect.[19] Eventually, the Achilles heel of vitrimers is the potential to creep under moderate use conditions. Pronounced creep behavior represents an important drawback that could prevent vitrimers from being developed for a wide variety of applications requiring robust network materials for applications demanding long-term dimensional stability (e.g., aerospace, building). Creep denotes the time-dependent relative deformation of a solid material under a constant force (tension, shear, or compression).[19] Various groups demonstrated substantially more creep of vitrimers than commercially available thermosets.[20−22] Even in some cases, pronounced creep is observed at temperatures slightly below T_v.[23,24] Indeed, for structural applications, temperatures below T_g are pivotal rather than high temperatures. Creep trials well below T_g suggest no significant difference of reference epoxy and epoxy vitrimer containing a certain fraction of permanent cross-links.[25] However, it is assumed that fast chemical reactions even stay relevant below a material's T_g although with a greater dependency on external forces to overcome diffusion restrictions.[26] In this light, molecular dynamic simulations indicate that higher stress loads might trigger dynamic bond exchange reactions even in the diffusion-controlled regime

yielding significantly more creep.[25] A promising approach to reduce creep is the integration of permanent cross-links.[16,20]

Ultimately, it is important that vitrimer resins not only meet the requirements in structural parts but also can be processed using established manufacturing processes, such as resin transfer molding. In concrete terms, this means that a sufficiently low viscosities (30−250 mPa·s[27−29]), sufficient pot life (time to reach the gelation point) for injection and fiber impregnation, and the curing cycle (time and temperature profile) must be compatible with established plant and tooling technologies. Such an approach can enable material recyclability and extend the lifetime of engineered parts directly contributing to sustainability.

Herein, we report the development of a high-performance epoxy resin, comparable to a commercially available aero-grade resin system, while being reprocessable, repairable, and recyclable. Therefore, we introduce a vitrimer resin based on a versatile platform that allows us to tailor resin systems up to a very high glass transition temperature of 195 °C. Incorporating a cardanol-based reactive diluent from a renewable feedstock broadens the reprocessing range to avoid significant degradation while plasticizing the network to counter the more brittle nature of the vitrimer resin. Further, different fractions of permanent cross-links are imbued into the network, and comprehensive studies on curing kinetics and gelation are carried out to construct conversion-temperature-phase (CTP) diagrams. Besides that, relaxation behavior, creep, and mechanical performance are accessed. Separate reprocessability and malleability studies are included to demonstrate the advantages of the developed vitrimer material.

2. MATERIALS AND METHODS

2.1. Materials. A two-component aero-grade qualified epoxy resin EPIKOTE 600 (EP 600) provided by Westlake Corp., consisting of part A (4,4′-methylenebis[N,N-bis(2,3-epoxypropyl)aniline]) and part B (4,4′-methylenebis(2,6-diisopropylaniline)), serves as a reference epoxy resin system. Part A of EP 600 provides the basis for the vitrimer formulation, which is provided in Table 1. Similar

Table 1. Mixing Ratios of the Different Formulations in Parts Per Weight (ppw) of the Resin Component

	EP 600 part A	EP 600 part B	4-AFD	513DF
EP	100	80		
VR	100		63	
VR-RD	70		63	30
VR 50-RD	70	40	31.5	30
VR 75-RD	70	20	47.3	30

well-established aero-grade resin systems (RTM 6 by Hexcel Corporation[30] and Cytec 890 RTM by Syensqo SA[31]) also rely on aniline platforms so that results presented within the present work might be applicable to a wide range of resin systems. Multifunctional biobased cardanol-derived reactive diluent LITE 513DF and 4-aminophenyl disulfide (4-AFD) are purchased from Cardolite Corp., and Molekula Ltd., U.K. Stoichiometries for the vitrimer and hybrid resin are back-calculated based on the mixing ratio provided by the manufacturer.

Thus, Li et al. postulate that hybrid polymer networks (bearing dynamic and permanent cross-links) remain fully reprocessable as long as the permanent cross-links are insufficient to form a percolated permanent network in the material.[20] Therefore, the network remains fully processable before reaching a critical conversion value at gelation ξ_{GP}[32] which is calculated to 0.33 according to the Flory−Stockmayer equation[33] (eq S1, Table S1). Based on the calculation, we imbue the
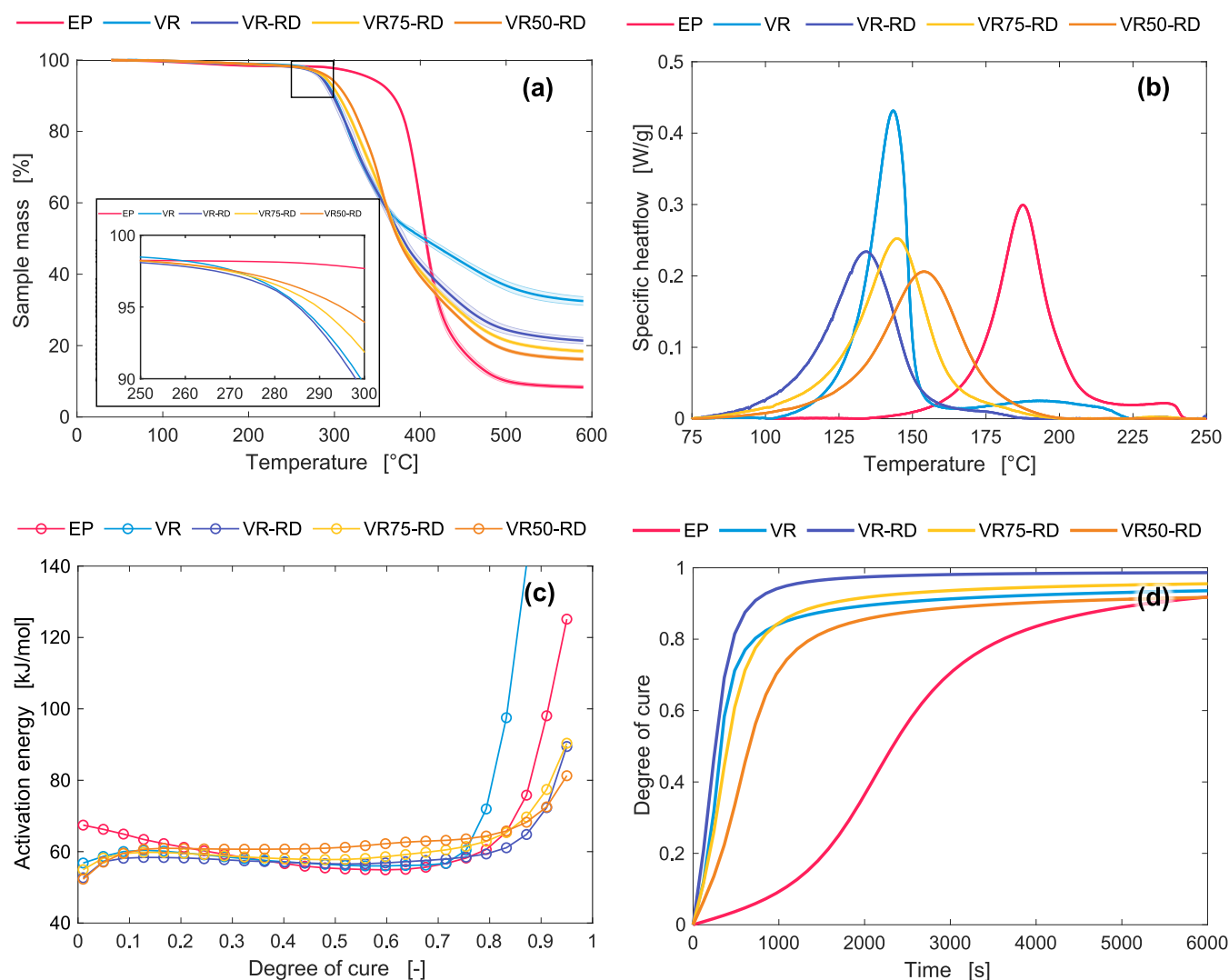
Figure 1. (a) Normalized sample mass during isothermal heating at 10 K/min. (b) Comparison of the heat flow of the different formulations at a heating rate of 1 K/min. (c) E_ξ dependency for the different resin formulations derived by the Friedman method. (d) Comparison of isothermal curing at 170 °C for the different resin formulations.

network with two different weight fractions of 25% (22 mol %, below ξ_{GP} threshold) and 50% (46 mol %, above ξ_{GP} threshold) of permanent cross-links that impart structural integrity. The objective is to ascertain how permanent cross-linking affects the characteristics and whether the beneficial properties of vitrimers can also be (partly) preserved above the threshold value. Although macroscopic flow with permanent bonds above ξ_{GP} is restricted, dynamic bond exchange may happen locally.

2.2. Characterization. Thermogravimetric analysis (TGA) is carried out to determine the degradation temperature T_d and maximum applicable measurement temperature while excluding any significant change in mass. Therefore, the change in mass during the DSC measurement in the temperature interval of 23−650 °C is first analyzed using TGA with a heating rate of 10 K/min. Small batches of 17 ± 2 mg are analyzed using TGA 4000 from PerkinElmer Corp.

Differential scanning calorimetry (DSC), a well-established method to analyze reaction kinetics, is selected to analyze the curing process based on the exothermal heat flow released during the curing reaction. The DSC analysis uses the mDSC250 device from TA Instruments, Inc. to analyze uncured liquid samples (Supporting Information). All measurements are carried out in a nitrogen atmosphere with 50 mL/min flow rates. Dynamic DSC scans with 1, 2, 4, 6, and 8 K/min are carried out at −50 to 250 °C (300 °C for the EP) temperature intervals to detect the initial glass transition temperature $T_{g,0}$ of the

uncured mixture and capture the heat flow during the curing reaction. Further, temperatures of 140, 160, and 180 °C are selected to characterize the isothermal curing process. The final glass transition temperature $T_{g,\infty}$ is determined after submitting the resin to an isothermal dwelling at 180 °C for 2 h. After subsequent cooling to 25 °C, modulated (1 K for 60 s) reheating to 250 °C at 4 K/min determines the $T_{g,\infty}$ of the samples.

A HAAKE MARS III rheometer (Thermo Fisher Scientific, Inc.) in parallel plate geometry, with a 20 mm diameter and a 1 mm gap, is used for the rheometry experiments. A temperature-controlled test chamber realized heating with temperature tolerances set to 0.1 °C. The sample preparation process is detailed in the Supporting Information. The initial steady-state shear viscosity of the individual formulation was measured by applying a constant controlled stress (CS mode) of 1 Pa and a heating rate of 2 K/min from 50 to 120 °C. For measuring the GP, isothermal measurements are conducted over a wide temperature range (four to five different temperatures ranging from 110 to 180 °C).

For the thermomechanical and mechanical analysis described in the following, neat resin specimens of different geometries were manufactured according to the methods described in the Supporting Information. Dynamic mechanical analysis (DMA) was performed with an RSA-G2 device from TA Instruments. Rectangular specimens ($9 \times 2 \times 25$ mm^3) were heated under air with 3 K/min from 30 to

250 °C. Measurements were performed in the bending mode with a static force of 0.01 N and a frequency of 1 Hz while applying a dynamic displacement of 7.5 μm (in the linear viscoelastic regime).

Relaxation trials under air were performed at different isotherms below (i) and above (ii) T_g. For (i), rectangular samples of ($9 \times 2 \times 25$ mm^3) were mounted in a three-point bending fixture. After reaching the requested temperatures of 40−180 °C (VR-RD, VR 75-RD, VR 50-RD) and 40−210 °C (EP, VR), soaking for 10 min allowed the system to achieve temperature equilibrium before applying a 0.1% strain and recording the stress for 10^3 s. For (ii), the film tensile clamp was utilized ($6 \times 1 \times 30$ mm^3), and an instantaneous stress of 1% was applied within 0.1 s at temperatures ranging from 200 to 240 °C. After allowing temperature equalization for 5 min, the decay in stress was recorded for 10^3 s.

Both reference resin and vitrimer formulations were tested by using creep experiments below T_g. Rectangular samples of ($6 \times 1 \times 30$ mm^2) were tested in the dual cantilever fixture. A stress of 10 MPa (12−15% of ultimate flexural strength (UFS)) was applied within 0.1 s at 30, 80, and 130 °C (to map potential operating temperatures), and the strain was monitored for 10^3 s.

Destructive mechanical testing based on the ASTM D790 standard was applied to investigate the flexural properties of the different resin formulations. A ZwickRoell universal testing machine with a 1 kN load cell mounted was used to test the specimens with a span width of 64 mm at a speed of 1 mm/min.

3. RESULTS AND DISCUSSION

3.1. Thermogravimetric Analysis. Figure 1a confirms the onset of degradation associated with a temperature ($T_{d,5\%}$) at which a 5% mass loss occurs. $T_{d,5\%}$ ranges from 285 °C (VR-RD) to 294 °C (VR 50-RD), which are in the range of high-T_g epoxy materials bearing disulfide bond (e.g., 285−291 °C[9,13]). Thermal stability increases when permanent bonds are incorporated into the formulations. This can be attributed to the diminished presence of disulfide species energetically less stable than carbon−carbon bonds.[34] Therefore, $T_{d,5\%}$ of the EP (341 °C) confirms an increased temperature stability compared with the disulfide formulations. Adding reactive diluent to the formulation decreases the degradation temperature slightly until it becomes more pronounced at temperatures greater than 350 °C, indicating a two-step degradation process corresponding to the premature decomposition of aliphatic side chains (≈350 °C) and the benzene rings (≈450 °C) of the cardanol-based reactive diluent[35] (Figure S1). Further, the vitrimer formulations show significantly higher char yields compared to the EP reference indicating higher cross-linking networks and more rigid chemical structures.

Based on TGA results, maximum temperatures of 250 °C (300 °C for the reference resin) are selected for further analysis (DSC, DMA) to exclude premature material degradation for all resin formulations during testing.

3.2. Reaction Kinetics. The total heat released during the curing reaction is captured in Table 2. We assume that the measured enthalpy corresponds only to the epoxy-amine curing response, as any energy exchange due to disulfide bond

exchange exhibits a zero net effect. A $\Delta H_{R,total}$ value of 456 J/g for the EP is in good agreement with a similar aniline-based resin reported in the literature (446 ± 9 J/g[36]).

Interestingly, VR shows significantly higher $\Delta H_{R,total}$ values, and the average exothermic peak temperature shifts to lower values (by up to 48 °C), indicating that the curing reaction of the vitrimer is already initiated at lower temperatures. Further, the total reaction enthalpy substantially increases by 22%. This increase can be explained by the differences in the chemical structures of the hardeners used, being diisopropylaniline-based structure for the reference resin and disulfide entailing structure for the 4-AFD possessing different electronic densities due to the aforementioned functional groups. The pronounced exothermal reaction might cause temperature peaks, especially for thick-walled components, yielding potential material degradation. That circumstance might become a threat concerning the limited temperature stability of aromatic disulfides (as some authors observed significant degradation even at temperatures below 220 °C[17,37]). It might, therefore, affect the reprocessability, recycling, and healing properties. Further, a pronounced exothermal reaction favors temperature gradients in the thickness direction, yielding aggravating residual stresses within the cured parts.[38] This circumstance is intensified by a considerably narrower specific heat flow peak, meaning that a significant amount of heat is released in only a short interval (Figure 1b). Further, for the EP and VR, small shoulders are observed, which might be explanation by competing reactions, i.e., epoxy-amine and epoxy-hydroxyl which give rise to two overlapping peaks in plots of heat flow against temperature. A comprehensive overview of the measured heat flows for the different heating rates and resin formulations can be obtained in Figure S2.

Incorporating the biobased reactive diluent decreases the total reaction enthalpy to an average of 463 J/g and broadens the peak while shifting the initiation of the reaction to lower temperatures. With an increasing fraction of epoxy hardener, the initiation and peak temperatures shift back to higher temperatures. This observation seems reasonable as reactivity is governed not only by the nature and structure of the hardener but also by the epoxy itself.[39] The structure of the epoxy and its substituents affect the reactivity between epoxy and amine moieties.[40]

Further, Friedman's isoconversional method (Supporting Information, eqs S2 and S3) is used to estimate the cure-dependent activation energy E_ξ of the curing process to provide insights into mechanistic analysis, detecting governing curing mechanisms.[41] The activation energies E_ξ (Figure 1c) confirm a more reactive behavior of VR-RD in the initial stage, exhibiting an activation energy of 52 kJ/mol, whereas the EP shows significantly higher values of 67 kJ/mol. Still, the activation energies of all formulations range from 50 to 70 kJ/mol in the liquid and rubbery region ($\xi < 0.8$), which is in the range of conventional epoxy-amine reactions and in the range for aromatic disulfide-containing epoxy vitrimers (55−80 kJ/mol).[18,37]

The continuous decrease of E_ξ between 0.2 and 0.6 degrees of cure can be attributed to the autocatalytic nature of the system. Surprisingly, the VR 50-RD does not show a decrease in activation energy, staying rather constant until 0.8 conversion. This might be attributed to the premature initiation of the disulfide reaction and is accompanied by an early-stage viscosity increase. With the proceeding curing reaction, the viscosity increases, enforcing more energy for

Table 2. Mean Peak Temperatures and Total Reaction Enthalpy Determined by DSC

	T_{peak} [°C]	$\Delta H_{R,total}$ [J/g]
EP	219 ± 24	456 ± 8
VR	171 ± 21	558 ± 8
VR-RD	164 ± 21	463 ± 13
VR 75-RD	174 ± 21	456 ± 4
VR 50-RD	185 ± 23	445 ± 13

motion among molecule chains even before initiating the reaction with the aniline hardener and therefore reducing the autocatalytic effect of the aniline hardener. Finally, above 0.8 conversion, the reaction becomes increasingly diffusion-dominated, generating long chains that hinder the mobility of the remaining monomers. In this region, the activation energy increases to values greater than 140 kJ/mol. The EP and VR tend to become diffusion-controlled at an earlier stage compared to the formulations containing reactive diluents and exhibiting a lower T_g.

As indicated in Figure 1c, the change of E_ξ emphasizes that the cross-linking exhibits a more complex behavior and involves multiple reaction mechanisms that require supplementary investigation. Therefore, a model-based kinetic model approach is selected to study the reaction kinetics. Model-based approaches are more versatile and able to simulate systems in which temperature history plays a role,[36] which might be relevant to postcuring analysis and combining isothermal dwelling and nonisothermal curing (as recommended by the manufacturer). For this, an advanced model-based approach (eqs S4−S9) that also considers diffusion is applied to approximate the curing behavior of all resin formulations. The detailed modeling is described in the Supporting Information. Tables S2 and S3 summarize the fitting parameters for the different resin systems. A comprehensive comparison of measurement data and model is provided in Figure S3. Mean average errors (MAE) below 3% (Table S3) indicate an excellent agreement of measurement data and model. It is important to note the striking differences between EP and VR in the pre-exponential factors A_1 and A_2 (cf. Table S2). VR exhibits substantially higher values for both A_1 and A_2, implying a stronger dependency on initiated and catalyzed reactions from H-donor molecules and a more decisive influence on internally catalyzed reactions from generated hydroxyl groups. Besides that, EP also shows a balanced contribution of both reactions but significantly lower values for A_1 and A_2. This difference emphasizes the higher reactivity of 4-AFD compared to the part B component of EP.

The glass transition temperature development during curing is depicted in Figure S4, and corresponding parameters are summarized in Table 3. Typically, T_g increases during curing,

Table 3. Parameters According to Eq S9

	λ	$T_{g,0}$ [°C]	$T_{g,\infty}$ [°C]	R^2
EP	0.57	−11.7	214.5	0.99
VR	0.37	−13.1	225.2	0.99
VR-RD	0.43	−15.9	184.2	0.99
VR 75-RD	0.45	−18.9	174.0	0.99
VR 50-RD	0.57	−18.7	175.2	0.99

at the same time yielding a higher cross-link density. For the investigated formulations, glass transition temperature initially ranges from −18.9 to −11.7 °C and develops up to final glass transition temperatures of 174.0−225.2 °C. Utilizing 4-AFD as a curing agent shifts $T_{g,\infty}$ to higher temperatures well above $T_{g,\infty}$ of the reference system, which might become a threat to (re)processing of the resin as the processing window ($T > T_{g,\infty}$) partly superimposes the degradation range, which might facilitate damaging the material. As expected, incorporating reactive diluent into the formulation decreases $T_{g,\infty}$ to 184 °C, which broadens the temperature range for initiating dynamic bond exchange.

Figure 1d compares the isothermal curing process of the different resin formulations based on the developed models. The pronounced differences of the various resin formulations concerning the reaction progress become apparent. As already indicated by the lower E_ξ values (cf. Figure 1c), VR-RD resin cures comparably faster than the other resin formulations. It becomes evident that increasing amounts of aniline hardener successively slow the curing reaction.

This circumstance becomes even more apparent when considering the cure rate (Figure S5). Since the cure rate is directly proportionate to the heat flow released, a significantly greater heat of reaction can be expected in a smaller time interval, which can cause large temperature gradients in thick-walled laminates, in particular, resulting in high residual stresses and the potential degradation of the material.

3.3. Viscosity Development. The rheometer measurements aim for two objectives: First, we evaluate the shear viscosity development of the different resin formulations with varying temperatures representing the conditions encountered during the injection and fiber impregnation processes in composite manufacturing. Second, isothermal dwellings at elevated temperatures capture the development of shear storage and loss modulus at a frequency of 1 Hz and allow the identification of the time to reach the gelation point (GP).

The temperature-dependent viscosity development of different resin formulations is provided in Figure 2a. The initial viscosity decreases with increasing temperature as a result of enhanced molecular mobility. Exchanging the hardener for 4-AFD (VR) increases the viscosity and makes liquid molding challenging, assuming a viscosity window of 30−250 mPa·s[27,28,31] for processing. Further, the more reactive nature of the disulfide-based systems (compared to the reference hardener) becomes evident, as a curing-induced increase in viscosity can be observed at temperatures above 100 °C.

By substitution of a part of the resin by reactive diluent, viscosity is shifted to lower values in the range of the reference resin, satisfying the processing requirements. The hybrid formulations (VR 75-RD, VR 50-RD) are located below the EP reference. Still, the shorter residual time of the VR needs to be considered which manifests at a more pronounced viscosity increase with time and a compressed processing window (Figure S6).

3.4. Gelation. Different rheological and dielectric evaluation methods have been proposed for detecting the GP. Indeed, the rheological-based Winter−Chambon criterion[42] is well established for determining the GP of EP. The criterion describes gelation as the frequency-independent point of time at which the loss factors of different frequencies intersect. Still, within the present work, we refrain from using the Winter−Chambon criterion and use the crossover of G' and G'' at 1 Hz to define the gelation point as suggested in refs 37,43 while ensuring curing temperatures exceed the glass transition temperatures at GP ($T > T_{g,GP} + 30$ °C) as proposed in ref 43. The gelation point of a thermosetting resin corresponds to the degree of cure at which the incipient percolated network forms. From an engineering perspective, this is a critical stage as the viscosity increases exponentially, restricting further processing. Additionally, the rapid increase of mechanical moduli at the GP initiates the development of most residual stresses in composite materials,[44,45] whereas stress development before gelation is minimal due to immediate relaxation. Typically, gelation is characterized by a temperature-
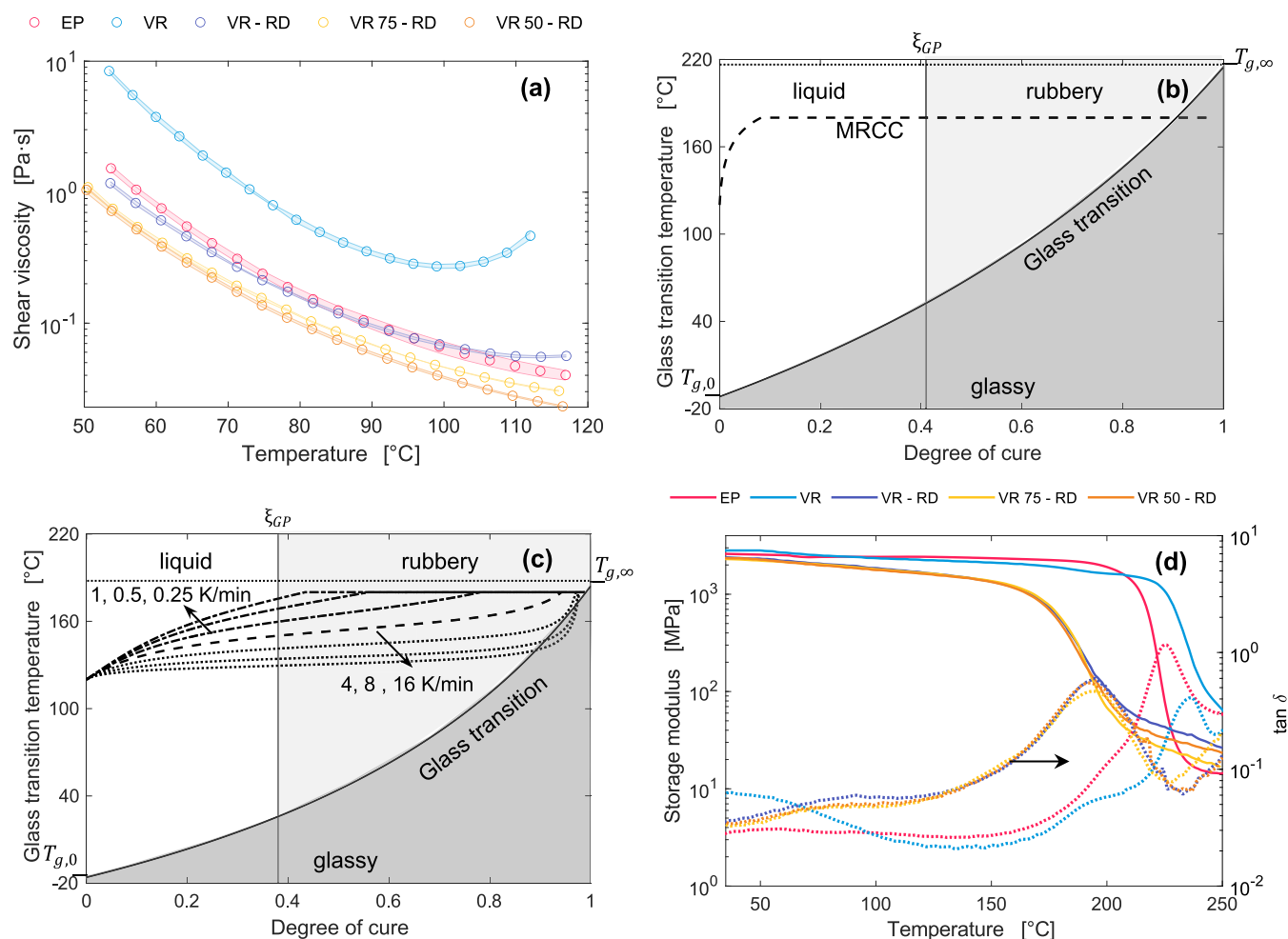
Figure 2. (a) Temperature-dependent shear viscosity of the different resin formulations. Conversion-temperature phase diagrams for EP (b) and VR-RD (c). Dashed lines indicate the MRCC (120−180 °C with 2 K/min and isothermal dwelling at 180 °C for 2 h), dotted lines indicate elevated heating rates, and dash-dotted lines indicate lower heating rates during the initial temperature ramp. CTP diagrams of the other resin formulations are provided in Figure S8. (d) Dynamic mechanical analysis at 3 K/min for the different resin formulations.

Table 4. Degree of Cure at Gelation ξ_{GP} for the Different Formulations Measured at Different Temperatures

Temperature [°C]	EP	VR	VR-RD	VR 75-RD	VR 50-RD
110			0.37		
120		0.31	0.35	0.42	0.41
130		0.33	0.38	0.39	0.42
140		0.36	0.39	0.41	0.43
150	0.37	0.39	0.39	0.44	0.44
160	0.42	0.39			
170	0.41				
180	0.43				
Average	0.41 ± 0.03	0.36 ± 0.03	0.38 ± 0.02	0.41 ± 0.02	0.43 ± 0.02
Calculation	0.32	0.35	0.4	0.39	0.39

independent degree of cure at gelation ξ_{GP} rather than a specific time.[46]

Combining rheological investigations and known reaction kinetics enables us to calculate ξ_{GP} solving eqs S5−S9 for the temperature profile recorded during the isothermal rheometer measurements. An initial degree of cure of 0.01−0.03 compensates for the minute that elapses between filling and closing the rheometer gap and starting the measurement.

Table 4 gives an overview of the calculated ξ_{GP} for the different resin formulations. Figure S7 provides the develop-

ment of the storage and loss modulus and cure development. Measured ξ_{GP} of EP exhibits values close to a similar system (RTM 6) reported in the literature.[47] Further, ξ_{GP} is calculated according to the Flory−Stockmayer equation (Table S1), yielding values of ξ_{GP} = 0.33−0.40 for the different resin formulations.

The calculations gave consistently lower values. The divergence between measurements and theoretical consideration may be attributed to the standard error of the kinetic model (cf. Table S3) and a slight difference between the

recorded and the actual temperature present within the resin specimen. Still, the differences are within the standard deviation for all resin systems apart from the EP. Slight deviations might be explained by a substitution effect in the amine group, with the secondary amine reacting at a slower rate than the primary amine, particularly for aromatic diamines[33] and intramolecular cyclization. Compared to the theoretical values, the gel point of our vitrimers is delayed compared to typical tetra-functional epoxy-diamine systems. High gel conversions have been described when deviations from the ideal stepwise cross-linking reaction occur.[48,49]

The vitrimer resins exhibit a higher average ξ_{GP} compared to that of the reference. Still, processing time significantly decreases for the VR as it cures faster (Figure 1d), providing less flexibility for the processing. For the EP, gelation occurs at 35 min, whereas VR-RD resin becomes rubbery after 5 min at temperatures of 170 °C, revealing the significant difference induced by the curing process.

3.5. Conversion-Temperature Phase Diagram.
Although time temperature transformation (TTT) plots have already been reported for vitrimers,[9,13,18,37] these exhibit the disadvantage of being only valid for isothermal cure conditions.[45] As the manufacturer recommended cure cycle (MRCC, 120−180 °C with 2 K/min and subsequent isothermal dwelling at 180 °C for 2 h) of the investigated reference resin and vitrimer formulations state a significant proportion in the nonisothermal region, conversion-temperature phase (CTP) are beneficial as these allow combining immediate reading of isothermal and dynamic cure conditions. Therefore, compiling reaction kinetics and gelation measurements enables us to construct CTP diagrams, according to Adabbo and Williams[50] depicted in Figure 2b,c.

First, one can identify that EP passes through the liquid region and reaches the rubbery state after the heating stage. The isothermal curing step proceeds mostly in the liquid rubbery regime, followed by vitrification and final diffusion-driven curing. Compared to the EP, the curing of the VR-RD resin proceeds significantly faster and favorably occurs during the heating step, while vitrification cannot be observed during curing, according to MRCC. Further, significantly decreasing the heating rate (Figure 2c) shifts the temperature at gelation to higher values and is beneficial to intercept temperature peaks caused by the accelerated exothermic curing process. Higher heating rates cause vitrification and subsequent devitrification and are not favorable as they might be accompanied by temperature and curing degree gradients within the part.

3.6. Dynamic Mechanical Analysis.
The thermomechanical behavior of the different resin systems is shown in Figure 2d. The values capture the average of three measurements. The solid-state moduli at 40 °C range from 2.8 (VR) to 2.4 GPa for the reactive diluent formulations. The measured modulus of the reference resins is closely related to the value reported in the technical data sheet (3.1 GPa).[28] Differences might be attributed to divergent boundaries during DMA and quasistatic flexural testing.[51] Although the differences in modulus at 40 °C are not as pronounced, a premature stiffness decline can be observed for formulations with reactive diluent content. The stiffness decreases by 40% in the temperature interval from 40 to 150 °C, whereas with VR and EP, it only amounts to 10%. This pronounced decrease might be related to the secondary β-relaxation that becomes active above 50 °C, indicated by a small tan δ-peak at 90 °C. A secondary β-relaxation mechanism

may occur below the glass transition temperature (α-relaxation),[52] involving the local motion of a flexible long-chain aliphatic group of reactive diluent that triggers the many-molecule cooperative glass transition. Similar behavior was reported for the incorporation of aliphatic reactive diluent into diglycidyl ether of bisphenol A.[53] Therefore, the cardanol-based reactive diluent induces a plasticizing effect, reducing stiffness by the β-relaxation of a smaller part of molecules.

Table 5 overviews the glass transition temperatures of the different resin formulations according to various criteria

Table 5. Glass Transition Temperatures of All Resin Formulations Determined by DMA

	$T_{g,in.}$ [°C]	$T_{g,mid}$ [°C]	T_g (E''_{max}) [°C]	T_g (tan δ_{max}) [°C]
EP	209.8	222.6	217.0	225.1
VR	223.8	234.1	227.7	234.9
VR-RD	161.2	183.3	178.4	194.5
VR 75-RD	167.3	181.6	175.9	192.1
VR 50-RD	157.8	180.4	174.6	193.1

(extrapolated onset temperature $T_{g,in}$, midpoint temperature of the storage modulus $T_{g,mid}$, temperature of maximum loss factor T_g (tan δ_{max}), and loss modulus E''_{max} T_g (E''_{max})). The measurement data confirm the correlation shown in Table 3. Utilizing 4-AFD as a hardener increases T_g and incorporating the reactive diluent reduces T_g significantly.

It is observed that the glass transition temperature decreases with added reactive diluent while the peak intensity increases. Matsuoka[54] states that an increased number of cross-linking points results in (i) reduced chain mobility, (ii) a loss of free volume, and (iii) an increase in T_g. In the present case, the reactive diluent linearizes the network structure and reduces the number of cross-linking points so that the T_g decreases. The intensity of the tan δ peaks directly relates to the extent of motion associated with the glass transition. Consequently, the more flexible structure of the network containing reactive diluent (lower storage modulus, Figure 2d) yields an increase in the tan δ peak intensity. Compared to the VR without reactive diluent, network structures with reactive diluent exhibit broader tan δ peaks, indicating a higher degree of microstructural heterogeneities.[55]

Indeed, adding the reactive diluent decreases the T_g. Still, we expect a more flexible network with increased plasticity that is beneficial for the malleability and reprocessing of the network. Furthermore, the lower T_g permits reprocessing at lower temperatures and thereby offers a decisive advantage; as for a similar vitrimer (T_g = 233 °C) reprocessing was limited by thermal degradation of the material.[9] Other authors are even more critical and postulate significant degradation (>25%) after 30 min at 210 °C.[17] For this reason, incorporating a reactive diluent can be advantageous as it broadens the (re)processing window.

3.7. Relaxation.
First, relaxation trials below T_g are discussed before focusing on the trials above T_g to qualify the bond exchange mechanism and determine the T_v. For an epoxy resin, different authors demonstrate that the temperature dependence of a_T can be well manifested by an Arrhenius relationship below T_g,[56] while above T_g, the well-known WLF[57] equation is the most appropriate.[58] Assuming no significant contribution of the dynamic bonds on the relaxation behavior below T_g, we approximate the epoxy vitrimers

relaxation by an Arrhenius-like approach previously applied for an epoxy resin:[58]

$$\log a_T = \frac{-E_a}{\ln 10 R}\left(\frac{1}{T} - \frac{1}{T_{ref}}\right) \qquad (1)$$

As the rate of change in the shift factors tends to be smaller in the temperature region below T_g,[56,57] we limit the temperature range to temperatures $T < T_g$. Further, constants obtained above T_g are not useful for predicting the material response for structural applications (necessarily operating below T_g) as a drastic change in activation energy is expected for higher temperatures where the effects of the glass transition become neglectable. Different authors demonstrated distinct shift factor regions which are either dominated by the dynamic bond exchange dynamics (at high temperatures) or the glassy dynamics at low temperatures.[59,60]

Figure S9 captures the master curves at a reference temperature of 35 °C and the determined shift factors, while the stress relaxation and shifted master curves are provided in Figure S10. The EP and VR curves show similar qualitative progressions and are run almost parallel. Still, at elevated temperatures, VR tends to relax significantly faster, which might be attributed to an extended contribution of the disulfide bond exchange dynamics close to the rubbery regime. Contrary to that, the glassy state overall dynamics (at lower temperatures) are controlled by the monomeric friction and the free volume of the network.[59] The formulations containing reactive diluents show smaller initial modulus values and faster stress relaxation attributable to a lower T_g and broader relaxation peak (cf. Figure 2d), activating the relaxation process at lower temperatures. Further, the permanent cross-links slightly decrease the stress relaxation rate, yielding a slower exponential decay. A similar correlation was observed for imbuing permanent cross-links into the vitrimer network based on transesterification.[20] Further, the Arrhenius fitting gives us activation energies ranging from 179 kJ/mol for VR-RD to 201 kJ/mol for VR 50-RD, confirming a higher energy barrier caused by the permanent cross-links.

Within this work, we use the well-established definition of topology freezing temperature (T_v), defined by the temperature at which the material reaches the liquid-to-glass transition (at a viscosity of 10^{12} Pa·s).[61] Hence, the transition from viscoelastic solid to viscoelastic liquid at T_v is calculated from the Maxwell relation for viscoelastic fluids for a relaxation time $\tau^* = \eta/G$, with G being the rubbery shear modulus and η the shear viscosity at the liquid-to-glass transition. As the rubbery shear modulus is not directly measured, G is calculated from the E' value in the rubbery region (obtained from DMA measurements, cf. Figure 2d), assuming homogeneous isotropic behavior and Poisson's ratio v of 0.5[62] in the rubbery state utilizing Lamé coefficients: $G = E'/(2(1+v))$.[63] While assuming Arrhenius-like behavior of the relaxation time τ according to eq 2,[64] T_v can be extrapolated at τ^*.

$$\tau(T) = \tau_0 \exp\left(\frac{E_a}{RT}\right) \qquad (2)$$

where τ represents the relaxation time at the absolute Temperature T, E_a is the activation energy of the bond exchange, and R is the universal gas constant (8.314 J mol^{-1} K^{-1}).

Table 6 and Figure 3a summarize the results of the stress relaxation above T_g. The normalized stress relaxation curves of

Table 6. Characteristic Values Derived from Stress Relaxation above T_g

	E_a [kJ mol^{-1}]	τ^* 10^5 [s]	T_v [°C]	R^2
VR-RD	125	5.88	89	0.97
VR 75-RD	140	6.67	110	0.99
VR 50-RD	149	8.57	124	0.99

the different resin formulations are provided in Figure S11. E_a and extrapolated T_v are in the range of vitrimers containing aromatic disulfide cross-links. Surprisingly, we state comparably low activation energy and T_v related to the high glass transition temperature vitrimers bearing aromatic disulfide bonds reported in the literature: (i) $T_g = 176$ °C, $E_a = 246$ kJ/mol and $T_v = 152$,[16] (ii) $T_g = 163$ °C, $E_a = 196$ kJ/mol and $T_v = 150$ °C.[14]

The VR-RD formulations show lower epoxy/amine ratios ($r = 0.8$) (Table S1) that could explain the reduced stress relaxation times. Some literature suggests catalytic activity of unreacted amines on S–S exchange could be the reason for faster stress relaxation.[12] A more straightforward hypothesis is that the higher concentration of dynamic hardener decreases relaxation times, plus the excess primary/secondary amines lead to lower cross-linking density, larger free volume, and more network mobility to facilitate S–S exchange.

Similar to the measurements below T_g, the permanent bonds in the network appear to decelerate the relaxation process. While this effect is not strongly pronounced in the glassy state, the influence of the permanent bonds above T_g plays a decisive role, as indicated by the relaxation times at 220 °C (Figure 3a). Also, the literature reports increased relaxation times of bond exchanges via transesterification by increasing the fraction of permanent cross-links.[20]

The increased cross-linking is also reflected in the final stress value: It is apparent that the VR 50-RD formulation exhibits a final normalized stress value of 28% (although the testing temperatures increased by 10 °C, no value below $1/e$ was reached at 210 °C) at the end of the relaxation measurements, while the other two formulations decline to 3 and 19% for the VR-RD and VR 75-RD, respectively (cf. Figure S11).

The vitrimer exhibits swift stress relaxation (5 s at 230 °C) and is a promising candidate for engineering malleable, healable, and recyclable composite applications. A decisive influence of the permanent bonds on the bond exchange dynamics and extrapolated T_v is demonstrated. The permanent bonds lead to significantly higher activation energies and T_v and contribute to longer relaxation times, which can be a potential drawback concerning the possible degradation of the disulfide bonds at elevated temperatures; but can also facilitate creep resistance. For high-performance applications, the exchange kinetics of vitrimer materials should be suppressed at the service temperature to avoid creep while promoting fast exchange at (re)processing temperatures.

3.8. Creep. Figure 3b,c depicts the creep behavior of the different resin formulations at temperatures of 50, 100, and 150 °C. Very similar creep profiles were obtained, confirming comparable creep resistance of vitrimers compared to that of thermoset counterparts (for at least 1000 s). The reference system shows comparably smaller strains as the modulus is higher (Figure 2d). Further, one needs to consider the greater temperature difference ($T - T_g$) as the final glass transition temperatures of the EP and VR are higher (cf. Table 5).
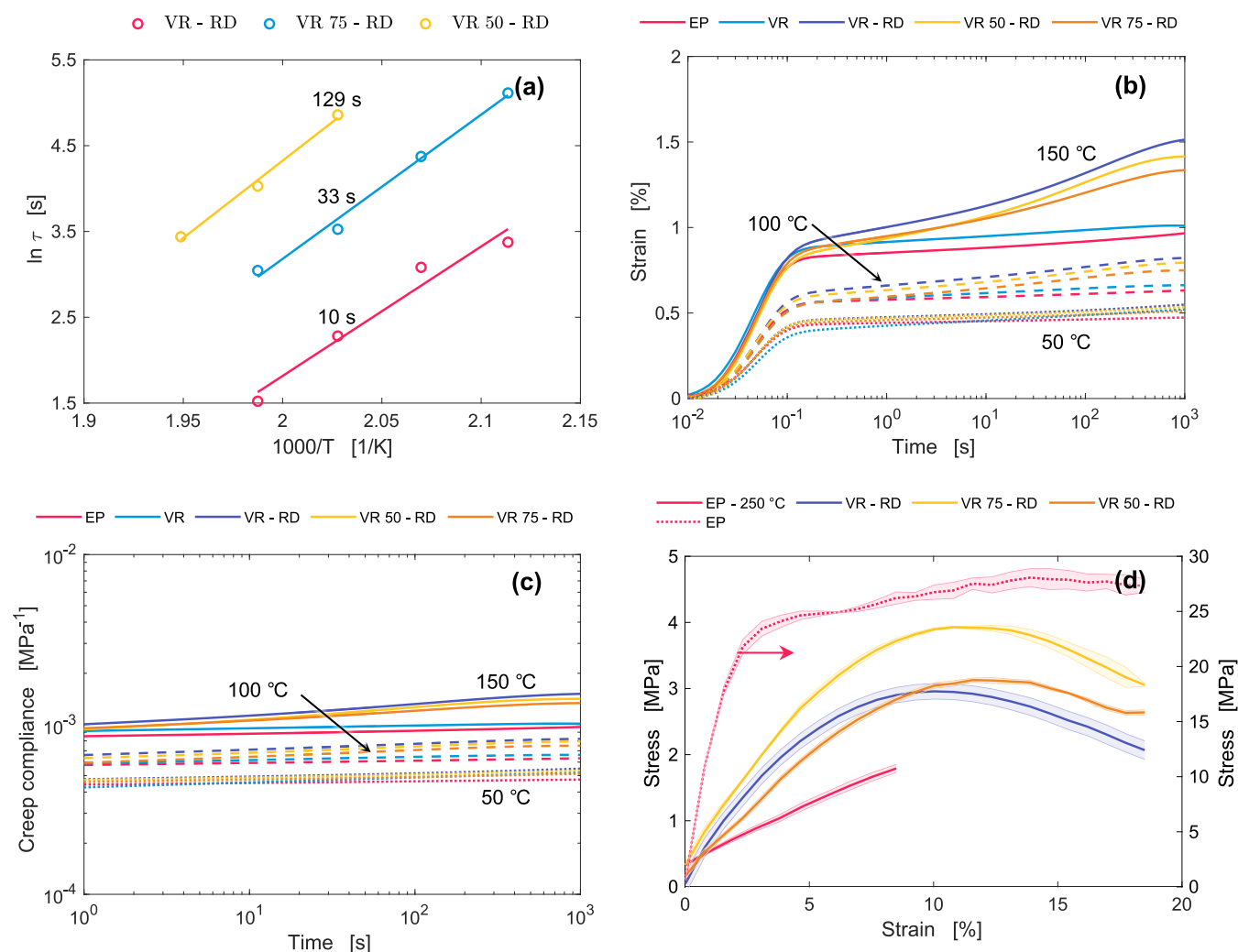
Figure 3. (a) Arrhenius plots of stress relaxation for the different resin formulations. Labels indicate relaxation times at 220 °C. Isothermal creep behavior at different temperatures (b) and creep compliance of the different resin formulations (c). (d) Strain−stress curves during reforming above T_g. Note the different y-axis for the EP at 200 and 250 °C.

Vitrimer resin systems behave similarly, and only slight differences can be identified. Below T_g creep is rather limited; therefore, exchange dynamics are of subordinate importance. Still, for 150 °C (T_g − 30 K) a slight increase in the creep compliance indicates several successful bond exchanges in the vitrimer, thus relaxing the stress accumulated in the network and exhibiting more considerable creep.[25] The vitrimer formulations may reach the secondary creep regime at high temperatures, superimposing two effects: elongation due to chain rearrangement (i) and sudden realignment of bonds orthogonal to the loading direction (ii), thus decreasing the stiffness along the loading axis and increasing the creep strain. Since the vitrimer formulations containing reactive diluents are already in the α-relaxation temperature range (cf. Figure 2d), subordinate network structures exhibit local mobility (enabling sudden realignment of bonds), even if the macroscopic cooperative glass transition is not fully triggered.

The results demonstrate only a minor influence of the permanent cross-links of 25 and 50% on the creep behavior at potential service temperatures, emphasizing the resin's potential for high-performance application. The pronounced creep of vitrimers (above T_g) discovered in various studies[20−23] appears to be of only minor importance below

the T_g, as does the number of dynamic bonds as also suggested based on molecular dynamic simulations.[25]

Although large-scale molecular motions (and pronounced creep) are triggered above T_g, the observed creep for both EP and vitrimer formulations may be attributed to the motions of very short segments of the polymer chains[65] being released after surpassing the β-transition (cf. Figure 2d, and observed at 50 °C for neat tetra-functional epoxy[66]). Therefore, at low temperatures, the vitrimers experience only small creep, never entering the superior creep regions as observed in ref 21, behaving as a traditional epoxy. We demonstrate that the designed vitrimer can arrest creep at temperatures up to 100 °C. The epoxy vitrimer exhibited almost no creep with strain values <0.8% at 100 °C (<1.5% at 150 °C) after 10^3 s at 12−15% of the UFS. This excellent creep resistance is comparable (at least for 10^3 s) to the creep response of conventional cross-linked networks such as the reference aero-grade epoxy resin.

3.9. Flexural Testing. Flexural testing tests were performed to characterize the mechanical properties and compare them with those of the reference resin (Figures S12 and S13 and Table 7). Substituting the EP 600 Part B component with the dynamic hardener increases the modulus and lowers the maximum strain, indicating a stiffer network.

Table 7. Flexural Properties of Different Resin Formulations

	$E_{0.25\%}$ [MPa]	σ_{max} [MPa]	ε_{max} [%]
EP	3215 ± 89	134 ± 13	7.7 ± 2.2
VR	3465 ± 96	117 ± 26	4.6 ± 1.6
VR-RD	3417 ± 149	122 ± 26	4.8 ± 1.5
VR 75-RD	3213 ± 75	145 ± 2	7.1 ± 1.2
VR 50-RD	3172 ± 37	141 ± 2	8.2 ± 2.3

Further, the maximum stress corresponds to the values for high-performance epoxy resins.[27,29] Still, one must consider the higher density of the vitrimer formulation (Figure S14), yielding reduced mechanical properties normalized by weight. Contrary to the expectations that excess of reactive diluents occupies the space between the reaction sites during curing and create many flexible segments, which induce the plasticizing effect in resin and decrease the tensile strength,[67] no distinct influence is observed in flexural load. Due to the highly aromatic and densely cross-linked nature of our system, we assume it would require more addition of linear segments to reach excess, leading to a decrease in tensile properties. Therefore, vitrimer and reference resin exhibit very similar properties and even become slightly stiffer. Merely, the elongation at break decreases significantly. Although this can be partially compensated for by the reactive solvent, complete recovery only occurs with 25% permanent cross-links.

Aviation components made from composite materials are often subjected to hydrothermal environments, which are known to impact the physical and mechanical properties of fiber-reinforced parts. Water absorption in epoxy resins alters their chemical and physical characteristics through mechanisms such as plasticization, crazing, hydrolysis, and swelling. Since epoxy resins are hydrophilic, we analyzed their water uptake based on the methods described in Figure S15. The results indicate that the vitrimer hardener reduces the amount of water absorption, offering a notable advantage over the reference material.

3.10. Demonstration of Mechanical Recycling and Malleability. Due to the expected challenge concerning thermal degradation of the disulfide bonds at temperatures well above 200 °C, we therefore refrain from further investigation of the malleability and recyclability of the VR (T_g = 234.9 °C) and limit ourselves to the formulations containing reactive diluents. First-generation specimens are comminuted by utilizing an electrical grinding unit to demonstrate the recyclability of the different vitrimer formulations. A sieve with a diameter of 1 mm ensured a defined upper limit of the particle. The mechanically comminuted shards were reconsolidated at temperatures of 200 °C ($\approx T_g + 5$ °C) while applying a pressure of 20 MPa in a metal mold (Figure S16). The reconsolidation demonstrates possible mechanical recycling and the profound self-healing of the vitrimer resins. The test specimens of the second generation are slightly distinguished visually from the test specimens of the first generation, as second-generation specimens exhibit inhomogeneous colorations representing the initial fragments (Figure S17).

Figure S18 shows the dynamic mechanical properties of all resin formulations before and after they go through the comminution and reconsolidation process at elevated temperatures. For the VR-RD, the T_g slightly reduces (by 4 °C), indicating some degradation occurring during the recycling process, which can be attributed to the mechanical damage of

the bonds by the intense comminution process or thermal degradation occurring during the reconsolidation.[16] Surprisingly, the T_g of the resin formulations bearing permanent cross-links increases to 199 °C (VR 75-RD) and 204 °C (VR 50-RD) respectively, which might be attributable to postcuring of the resin, not having reacted fully during the initial curing. Therefore, curing continues after submitting to temperatures above the initial T_g. Unfortunately, degradation of the bonds due to comminution and thermal degradation, as also observed with VR-RD, can not be excluded. Furthermore, it is astonishing that the VR 50-RD formulation can be reconsolidated, even though this should actually be ruled out according to theoretical considerations (Table S1, cf. Section 2.1). However, a noticeable difference can be observed between the test specimens: Although the shaped beams can be tested in the DMA, the individual grains are still clearly recognizable (Figure S17), so a significantly reduced performance can be expected for measurement methods that include not only stiffness but also performance at larger strains.

Further, 3-point pending specimens (10 mm spacing) of the vitrimer formulations are deformed with 1 mm/min at 200 and 250 °C for reference resin to demonstrate malleability (Figure S19). The recorded stress−strain curves are shown in Figure 3d. First, it should be mentioned that reshaping is possible for all vitrimer formulations, showing high strains of up to 18%. Indeed, at very high strains, the bending specimens first start to slide in the 3-point bending fixture (ε > 10%), reducing the force and subsequently contact the upper mandrel (ε > 18%), yielding a stress increase as demonstrated in Figure S19. Even if this prevents the test from being valid according to the standard, it allows a qualitative comparison of the reforming behavior of the resins. Repeating the same experiments with the reference resin at temperatures of 250 °C is not feasible, as even at low stresses, the resin breaks due to the absence of dynamic bonds. Still, the lower rubbery modulus of EP (c.f. Figure 2d) yields very small stresses.

The stress recorded during the deformation at 200 °C of the ER is significantly greater than that of the vitrimers and demonstrates the influence of the dynamic bonds; however, the significantly higher modulus of the ER at 200 °C ($T < T_g$, Figure 2d) must be considered. The formulation with 25% permanent cross-links (VR 75-RD) increases the resistance of the material to deformation. Increased stiffness is observed, which might be associated with the reduced amount of dynamic bond exchanges and the higher bond relaxation time (Figure 3a), yielding reduced fluidity of the network.

Contrary to expectation, VR 50-RD remains reformable at low stresses and decreased stiffness compared to the VR-RD network is reported. The network (containing subordinate networks of permanent cross-links within a continuous phase dynamic bond network) has only a limited resistance (caused by the reduced number of dynamic bonds) so that many-molecule cooperative movement of the oligomeric network is enabled with less resistance to external forces. This type of phase separation of covalent adaptable networks has been previously reported in the literature.[68,69] In detail, Song et al. demonstrate that even very low concentrations of dynamic bonds, well below the theoretical predicted value according to the Flory−Stockmayer equation, maintain reprocessing and self-healing capabilities. The authors hypothesize that viscosity difference of the two utilized epoxy monomers facilitates the formation of polymer chains containing dynamic covalent bonds that form continuous phases in the network even when

their concentration is less than 20 mol %.[69] Indeed, a distinct variation in viscosity can be observed for the monomers we used: 20 mPa·s at 80 °C measured for the reactive diluent and 350 mPa·s at 80 °C for the reference epoxy (Figure S20). Thus, we suspect a subordinate network of permanent cross-links within a continuous phase dynamic bond network, which enables reprocessing and self-healing capabilities even with dynamic bond fractions below the threshold value according to the Flory−Stockmayer equation.

4. CONCLUSIONS

Within the present investigation, we report the development of a high-performance epoxy resin with a very high glass temperature of 195 °C based on diglycidyl aniline, which is widely used in aero-grade resin systems. The processability (viscosity, cure cycle) can be tailored by incorporating reactive diluent based on renewable feedstock and different fractions of permanent cross-links into the formulation. Comprehensive studies of physicochemical, thermo-rheological, and curing reactions are carried out and summarized in a conversion-temperature phase diagram first reported for a vitrimer resin. Substituting the permanent bonds with the dynamic ones does not significantly affect the degree of cure at transitions (gelation and vitrification) but significantly accelerates the reaction so that a large part of the reaction, compared with the reference, occurs during the initial heating ramp in the MRCC.

Replacing the permanent hardener with a dynamic analogue did not significantly alter the mechanical properties of the resulting materials, although the vitrimer material tends to be slightly more brittle. However, this tendency can efficiently be counteracted by the reactive diluent and permanent cross-links. Very short relaxation times make the resin a very promising candidate for engineering malleable, healable, and recyclable composite applications. A decisive influence of the permanent bonds on the bond exchange dynamics and the extrapolated T_v is demonstrated, yielding longer relaxation times. We demonstrate that the designed vitrimer can arrest creep at temperatures up to 100 °C, comparable to the creep response of conventional cross-linked networks such as the reference aero-grade epoxy resin (at least for 10^3 s). Challenges concerning a narrow processing window that have been reported in the literature were met, demonstrating the malleability and reconsolidation of the specimens after mechanical comminution. All of the materials show great reformability, even with fractions of cross-links above the theoretical limit for GP. Still, systems with high fractions of permanent cross-links pose challenges during the reconsolidation process. The presented results represent an essential prerequisite to guide the application of disulfide-based vitrimer systems to individual processing conditions and set the scene for the development of vitrimer epoxy matrix-based composites.

ASSOCIATED CONTENT

Data Availability Statement

The data that support the findings of this study are available from the corresponding author upon reasonable request.

ⓈＩ Supporting Information

The Supporting Information is available free of charge at https://pubs.acs.org/doi/10.1021/acsapm.4c03731.

Calculation of ξ_{GP} from Flory−Stockmayer equation (Table S1, eq S1); specimen manufacture and sample preparation; thermogravimetric analysis (Figure S1); model free kinetics (eqs S2 and S3); heat flow recorded during DSC measurement (Figure S2); kinetic modeling of the curing reaction (Tables S2 and S3, Figures S3−S5, eqs S4−S9); development of the shear viscosity at different temperatures (Figure S6); rheokinetic determination of the gelation point (Figure S7); conversion-temperature phase (CTP) diagrams (Figure S8); stress relaxation below the glass transition temperature and master curves (Figures S9 and S10); stress relaxation above the glass transition temperature (Figure S11); flexural testing (Figures S12 and S13); density measurement (Figure S14, eq S10); water uptake (Figure S15); mechanical recycling and malleability (Figures S16−S19), and shear viscosity of epoxy monomers (Figure S20) (PDF)

■ AUTHOR INFORMATION

Corresponding Author

Niklas Lorenz − *Aerospace Structures & Materials Department, Faculty of Aerospace Engineering, Delft University of Technology, 2629 HS Delft, The Netherlands;* ⓞ orcid.org/0000-0003-1275-2579; Email: n.lorenz@tudelft.nl

Authors

William E. Dyer − *Aerospace Structures & Materials Department, Faculty of Aerospace Engineering, Delft University of Technology, 2629 HS Delft, The Netherlands*

Baris Kumru − *Aerospace Structures & Materials Department, Faculty of Aerospace Engineering, Delft University of Technology, 2629 HS Delft, The Netherlands;* ⓞ orcid.org/0000-0002-1203-4019

Complete contact information is available at:
https://pubs.acs.org/10.1021/acsapm.4c03731

Author Contributions

N.L.: Conceptualization, data curation, formal analysis, investigation, methodology, validation, visualization, writing—original draft, writing—review and editing. W.E.D.: Investigation, methodology, writing—review and editing. B.K.: Conceptualization, funding acquisition, writing—review and editing.

Notes

The authors declare no competing financial interest.

■ REFERENCES

(1) Alabiso, W.; Schlögl, S. The Impact of Vitrimers on the Industry of the Future: Chemistry, Properties and Sustainable Forward-Looking Applications. *Polymers* **2020**, *12* (8), 1660.

(2) Kumar, S.; Krishnan, S.; Prabakaran, K. Renewable Resource-Based Epoxy Vitrimer Composites for Future Application: A Comprehensive Review. *ACS Sustainable Resour. Manage.* **2024**, *1* (9), 2086−2107.

(3) Liu, Y.; Yu, Z.; Wang, B.; Li, P.; Zhu, J.; Ma, S. Closed-Loop Chemical Recycling of Thermosetting Polymers and Their Applications: A Review. *Green Chem.* **2022**, *24* (15), 5691−5708.

(4) Memon, H.; Wei, Y.; Zhu, C. Recyclable and Reformable Epoxy Resins Based on Dynamic Covalent Bonds − Present, Past, and Future. *Polym. Test.* **2022**, *105*, No. 107420.

(5) Lorenz, N.; Zawadzki, T.; Keller, L.; Fuchs, J.; Fischer, K.; Hopmann, C. Characterization and Modeling of an Epoxy Vitrimer Based on Disulfide Exchange for Wet Filament Winding Applications. *Polym. Eng. Sci.* **2024**, *64* (8), 3682−3702.

(6) Dyer, W. E.; Kumru, B. Polymers as Aerospace Structural Components: How to Reach Sustainability? *Macromol. Chem. Phys.* **2023**, *224* (24), No. 2300186.

(7) Fan, X.; Zheng, J.; Yeo, J. C. C.; Wang, S.; Li, K.; Muiruri, J. K.; Hadjichristidis, N.; Li, Z. Dynamic Covalent Bonds Enabled Carbon Fiber Reinforced Polymers Recyclability and Material Circularity. *Angew. Chem., Int. Ed.* **2024**, *63* (40), No. e202408969.

(8) Jagtap, A. R.; More, A. Developments in Reactive Diluents: A Review. *Polym. Bull.* **2022**, *79* (8), 5667−5708.

(9) Schenk, V.; D'Elia, R.; Olivier, P.; Labastie, K.; Destarac, M.; Guerre, M. Exploring the Limits of High-T(g) Epoxy Vitrimers Produced through Resin-Transfer Molding. *ACS Appl. Mater. Interfaces* **2023**, *15* (39), 46357−46367.

(10) Aranberri, I.; Landa, M.; Elorza, E.; Salaberria, A. M.; Rekondo, A. Thermoformable and Recyclable CFRP Pultruded Profile Manufactured from an Epoxy Vitrimer. *Polym. Test.* **2021**, *93*, No. 106931.

(11) Glass transition temperature testing of composites. https://www.compositesworld.com/articles/glass-transition-temperature-testing-of-composites (accessed October 31, 2024).

(12) de Luzuriaga, A. R.; Solera, G.; Azcarate-Ascasua, I.; Boucher, V.; Grande, H.-J.; Rekondo, A. Chemical Control of the Aromatic Disulfide Exchange Kinetics for Tailor-Made Epoxy Vitrimers. *Polymer* **2022**, *239*, No. 124457.

(13) Schenk, V.; De Calbiac, J.; D'Elia, R.; Olivier, P.; Labastie, K.; Destarac, M.; Guerre, M. Epoxy Vitrimer Formulation for Resin Transfer Molding: Reactivity, Process, and Material Characterization. *ACS Appl. Polym. Mater.* **2024**, *6* (10), 6087−6095.

(14) Anagwu, F. I.; Skordos, A. A. Cure Kinetics, Glass Transition Advancement and Chemo-Rheological Modelling of an Epoxy Vitrimer Based on Disulphide Metathesis. *Polymer* **2023**, *288*, No. 126427.

(15) Hao, C.; Liu, T.; Liu, W.; Fei, M.; Shao, L.; Kuang, W.; Simmons, K. L.; Zhang, J. Recyclable CFRPs with Extremely High Tg: Hydrothermal Recyclability in Pure Water and Upcycling of the Recyclates for New Composite Preparation. *J. Mater. Chem. A* **2022**, *10* (29), 15623−15633.

(16) de Luzuriaga, A. R.; Markaide, N.; Salaberria, A. M.; Azcune, I.; Rekondo, A.; Grande, H. J. Aero Grade Epoxy Vitrimer towards Commercialization. *Polymers* **2022**, *14* (15), 3180.

(17) Fanlo, P.; de Luzuriaga, A. R.; Albizu, G.; Ximenis, M.; Rekondo, A.; Grande, H. J.; Sardon, H. Unraveling the Thermal Stability of Aromatic Disulfide Epoxy Vitrimers: A Comprehensive Study Using Principal Component Analysis (PCA). *RSC Appl. Polym.* **2024**, *2* (5), 826−837.

(18) Sanchez-Rodriguez, D.; Zaidi, S.; Jahani, Y.; de Luzuriaga, A. R.; Rekondo, A.; Maimi, P.; Farjas, J.; Costa, J. Processability and Reprocessability Maps for Vitrimers Considering Thermal Degradation and Thermal Gradients. *Polym. Degrad. Stab.* **2023**, *217*, No. 110543.

(19) Van Krevelen, D. W.; Te Nijenhuis, K. *Properties of Polymers*; Van Krevelen, D. W.; Te Nijenhuis, K., Eds.; Elsevier: Amsterdam, 2009.

(20) Li, L.; Chen, X.; Jin, K.; Torkelson, J. M. Vitrimers Designed Both To Strongly Suppress Creep and To Recover Original Cross-Link Density after Reprocessing: Quantitative Theory and Experiments. *Macromolecules* **2018**, *51* (15), 5537−5546.

(21) Hubbard, A. M.; Ren, Y.; Picu, C. R.; Sarvestani, A.; Konkolewicz, D.; Roy, A. K.; Varshney, V.; Nepal, D. Creep Mechanics of Epoxy Vitrimer Materials. *ACS Appl. Polym. Mater.* **2022**, *4* (6), 4254−4263.

(22) Bin Rusayyis, M. A.; Torkelson, J. M. Reprocessable Covalent Adaptable Networks with Excellent Elevated-Temperature Creep Resistance: Facilitation by Dynamic, Dissociative Bis(Hindered Amino) Disulfide Bonds. *Polym. Chem.* **2021**, *12* (18), 2760−2771.

(23) Capelot, M.; Unterlass, M. M.; Tournilhac, F.; Leibler, L. Catalytic Control of the Vitrimer Glass Transition. *ACS Macro Lett.* **2012**, *1* (7), 789−792.

(24) Yang, Z.; Wang, Q.; Wang, T. Dual-Triggered and Thermally Reconfigurable Shape Memory Graphene-Vitrimer Composites. *ACS Appl. Mater. Interfaces* **2016**, *8* (33), 21691−21699.

(25) Perego, A.; Khabaz, F. Creep and Recovery Behavior of Vitrimers with Fast Bond Exchange Rate. *Macromol. Rapid Commun.* **2023**, *44* (1), No. 2200313.

(26) Van Lijsebetten, F.; Debsharma, T.; Winne, J. M.; Du Prez, F. E. A Highly Dynamic Covalent Polymer Network without Creep: Mission Impossible? *Angew. Chem., Int. Ed.* **2022**, *61* (48), No. e202210405.

(27) Hexcel Corp. Technical Data Sheet, RTM 6.

(28) Westlake Chemical Corp. Technical Data Sheet, Epikote System 600-2.

(29) Syensqo SA. Technical Data Sheet, Cycom 890 RTM Resin.

(30) Parsons, A. J.; Gonciaruk, A.; Zeng, X.; Thomann, F. S.; Schubel, P.; Lorrillard, J.; Johnson, M. S. Controlling Mass Loss from RTM6 Epoxy Resin under Simulated Vacuum Infusion Conditions. *Polym. Test.* **2022**, *107*, No. 107473.

(31) Syensqo SA. Safety Data Sheet, Cycom 890 RTM Resin.

(32) Flory, P. J. Molecular Size Distribution in Three Dimensional Polymers. I. Gelation. *J. Am. Chem. Soc.* **1941**, *63* (11), 3083−3090.

(33) Pascault, J.-P.; Williams, R. J. J. Overview of Thermosets: Present and Future. In *Thermosets*; Elsevier, 2018; pp 3−34.

(34) de Luzuriaga, A. R.; Martin, R.; Markaide, N.; Rekondo, A.; Cabañero, G.; Rodríguez, J.; Odriozola, I. Epoxy Resin with Exchangeable Disulfide Crosslinks to Obtain Reprocessable, Repairable and Recyclable Fiber-Reinforced Thermoset Composites. *Mater. Horiz.* **2016**, *3* (3), 241−247.

(35) Su, Y.; Zhang, S.; Zhou, X.; Yang, Z.; Yuan, T. A Novel Multi-Functional Bio-Based Reactive Diluent Derived from Cardanol for High Bio-Content UV-Curable Coatings Application. *Prog. Org. Coat.* **2020**, *148*, No. 105880.

(36) Skordos, A. A.; Partridge, I. K. Cure Kinetics Modeling of Epoxy Resins Using a Non-parametric Numerical Procedure. *Polym. Eng. Sci.* **2001**, *41* (5), 793−805.

(37) Sanchez-Rodriguez, D.; Zaidi, S.; Carreras, L.; de Luzuriaga, A. R.; Rekondo, A.; Costa, J.; Farjas, J. Time-Temperature-Transformation Diagrams from Isoconversional Kinetic Analyses Applied to the Processing and Reprocessing of Vitrimers. *Thermochim. Acta* **2024**, *736*, No. 179744.

(38) Sorrentino, L.; Polini, W.; Bellini, C. To Design the Cure Process of Thick Composite Parts: Experimental and Numerical Results. *Adv. Compos. Mater.* **2014**, *23* (3), 225−238.

(39) Malburet, S.; Bertrand, H.; Richard, C.; Lacabanne, C.; Dantras, E.; Graillot, A. Biobased Epoxy Reactive Diluents Prepared from Monophenol Derivatives: Effect on Viscosity and Glass Transition Temperature of Epoxy Resins. *RSC Adv.* **2023**, *13* (22), 15099−15106.

(40) Mora, A.-S.; Tayouo, R.; Boutevin, B.; David, G.; Caillol, S. A Perspective Approach on the Amine Reactivity and the Hydrogen Bonds Effect on Epoxy-Amine Systems. *Eur. Polym. J.* **2020**, *123*, No. 109460.

(41) Sbirrazzuoli, N. Determination of Pre-Exponential Factors and of the Mathematical Functions f(α) or G(α) That Describe the Reaction Mechanism in a Model-Free Way. *Thermochim. Acta* **2013**, *564*, 59−69.

(42) Chambon, F.; Winter, H. H. Linear Viscoelasticity at the Gel Point of a Crosslinking PDMS with Imbalanced Stoichiometry. *J. Rheol.* **1987**, *31* (8), 683−697.

(43) Tung, C. M.; Dynes, P. J. Relationship between Viscoelastic Properties and Gelation in Thermosetting Systems. *J. Appl. Polym. Sci.* **1982**, *27* (2), 569−574.

(44) O'Brien, D. J.; Mather, P. T.; White, S. R. Viscoelastic Properties of an Epoxy Resin during Cure. *J. Compos. Mater.* **2001**, *35* (10), 883−904.

(45) Müller-Pabel, M.; Rodríguez Agudo, J. A.; Gude, M. Measuring and Understanding Cure-Dependent Viscoelastic Properties of Epoxy Resin: A Review. *Polym. Test.* **2022**, *114*, No. 107701.

(46) Shimkin, A. A. Methods for the Determination of the Gel Time of Polymer Resins and Prepregs. *Russ. J. Gen. Chem.* **2016**, *86* (6), 1488−1493.

(47) Lionetto, F.; Moscatello, A.; Maffezzoli, A. Effect of Binder Powders Added to Carbon Fiber Reinforcements on the Chemo-rheology of an Epoxy Resin for Composites. *Composites, Part B* **2017**, *112*, 243−250.

(48) Tanaka, Y.; Stanford, J. L.; Stepto, R. Interpretation of Gel Points of an Epoxy-Amine System Including Ring Formation and Unequal Reactivity: Measurements of Gel Points and Analyses on Ring Structures. *Macromolecules* **2012**, *45* (17), 7197−7205.

(49) Matějka, L. Amine Cured Epoxide Networks: Formation, Structure, and Properties. *Macromolecules* **2000**, *33* (10), 3611−3619.

(50) Adabbo, H. E.; Williams, R. J. J. The Evolution of Thermosetting Polymers in a Conversion−Temperature Phase Diagram. *J. Appl. Polym. Sci.* **1982**, *27* (4), 1327−1334.

(51) Deng, S.; Hou, M.; Ye, L. Temperature-Dependent Elastic Moduli of Epoxies Measured by DMA and Their Correlations to Mechanical Testing Data. *Polym. Test.* **2007**, *26* (6), 803−813.

(52) White, S. R.; Mather, P. T.; Smith, M. J. Characterization of the Cure-state of DGEBA-DDS Epoxy Using Ultrasonic, Dynamic Mechanical, and Thermal Probes. *Polym. Eng. Sci.* **2002**, *42* (1), 51−67.

(53) Urbaczewski-Espuche, E.; Galy, J.; Gerard, J.; Pascault, J.; Sautereau, H. Influence of Chain Flexibility and Crosslink Density on Mechanical Properties of Epoxy/Amine Networks. *Polym. Eng. Sci.* **1991**, *31* (22), 1572−1580.

(54) Matsuoka, S. *Relaxation Phenomena in Polymers*; Hanser Publishers: Munich, 1992.

(55) Núñez-Regueira, L.; Villanueva, M.; Fraga-Rivas, I. Effect of a Reactive Diluent on the Curing and Dynamomechanical Properties of an Epoxy-Diamine System. *J. Therm. Anal. Calorim.* **2006**, *86* (2), 463−468.

(56) Nunes, S. G.; Saseendran, S.; Joffe, R.; Amico, S. C.; Fernberg, P.; Varna, J. On Temperature-Related Shift Factors and Master Curves in Viscoelastic Constitutive Models for Thermoset Polymers. *Mech. Compos. Mater.* **2020**, *56* (5), 573−590.

(57) Williams, M. L.; Landel, R. F.; Ferry, J. D. The Temperature Dependence of Relaxation Mechanisms in Amorphous Polymers and Other Glass-Forming Liquids. *J. Am. Chem. Soc.* **1955**, *77* (14), 3701−3707.

(58) Courtois, A.; Hirsekorn, M.; Benavente, M.; Jaillon, A.; Marcin, L.; Ruiz, E.; Lévesque, M. Viscoelastic Behavior of an Epoxy Resin during Cure below the Glass Transition Temperature: Character-ization and Modeling. *J. Compos. Mater.* **2019**, *53* (2), 155−171.

(59) Snijkers, F.; Pasquino, R.; Maffezzoli, A. Curing and Viscoelasticity of Vitrimers. *Soft Matter* **2017**, *13* (1), 258−268.

(60) Meng, F.; Saed, M. O.; Terentjev, E. M. Rheology of Vitrimers. *Nat. Commun.* **2022**, *13* (1), No. 5753.

(61) Montarnal, D.; Capelot, M.; Tournilhac, F.; Leibler, L. Silica-like Malleable Materials from Permanent Organic Networks. *Science* **2011**, *334* (6058), 965−968.

(62) Saseendran, S.; Wysocki, M.; Varna, J. Cure-State Dependent Viscoelastic Poisson's Ratio of LY5052 Epoxy Resin. *Adv. Manuf.: Polym. Compos. Sci.* **2017**, *3* (3), 92−100.

(63) Azcune, I.; Huegun, A.; de Luzuriaga, A. R.; Saiz, E.; Rekondo, A. The Effect of Matrix on Shape Properties of Aromatic Disulfide Based Epoxy Vitrimers. *Eur. Polym. J.* **2021**, *148*, No. 110362.

(64) Mechanical and Dielectric Response. In *The Physics of Polymers: Concepts for Understanding Their Structures and Behavior*; Strobl, G., Ed.; Springer: Berlin, 2007; pp 223−286.

(65) Feng, C.-W.; Keong, C.-W.; Hsueh, Y.-P.; Wang, Y.-Y.; Sue, H.-J. Modeling of Long-Term Creep Behavior of Structural Epoxy Adhesives. *Int. J. Adhes. Adhes.* **2005**, *25* (5), 427−436.

(66) Peterson, R. S.; Brandenburg, C. J.; Hinkley, J. A.; Gordon, K. L.; Thibeault, S. A.; Kang, J. H. Epoxy Resins with Reduced Viscoelastic Relaxation 2022 https://ntrs.nasa.gov/citations/20210021369 (accessed October 18, 2024).

(67) Sinha, A.; Islam Khan, N.; Das, S.; Zhang, J.; Halder, S. Effect of Reactive and Non-Reactive Diluents on Thermal and Mechanical Properties of Epoxy Resin. *High Perform. Polym.* **2018**, *30* (10), 1159−1168.

(68) De Heer Kloots, M. H. P.; Schoustra, S. K.; Dijksman, J. A.; Smulders, M. M. J. Phase Separation in Supramolecular and Covalent Adaptable Networks. *Soft Matter* **2023**, *19* (16), 2857−2877.

(69) Song, Z.; Wang, Z.; Cai, S. Mechanics of Vitrimer with Hybrid Networks. *Mech. Mater.* **2021**, *153*, No. 103687.